JOURNAL OF GUIDANCE, CONTROL, AND DYNAMICS
Vol. 29, No. 1, January–February 2006

Decentralized Control of Satellite Clusters Under Limited Communication

Gene M. Belanger,* Slava Ananyev,† and Jason L. Speyer‡
University of California, Los Angeles, Los Angeles, California 90095
David F. Chichka§
George Washington University, Washington, D.C. 20052
and
J. Russell Carpenter¶
NASA Goddard Space Flight Center, Greenbelt, Maryland 20771

Two decentralized control algorithms, each employing a unique information exchange scheme, are considered. One of these algorithms employs a communication paradigm in which control and local state estimate information is exchanged between members of a formation after any one of the members executes a control. The other algorithm requires only that control information be exchanged between members; this is thought to be the least information exchange that can sustain an affine control law. The performance of these algorithms when applied to a satellite formation control problem is evaluated. To this end, the algorithms are applied in the context of a nonlinear satellite cluster simulation, where Earth oblateness effects and measurement uncertainties are taken into account. The cluster is required to achieve a specified formation at a defined point on an elliptic reference orbit. Simulation results are obtained for several different orbits and compared to a baseline case involving a centralized controller design.

I. Introduction

CURRENTLY, there is much interest in the deployment of satellite formations to carry out activities such as Earth imaging, astronomical observations, and other scientific and military endeavors (Chichka,[1] Hughes and Hall,[2] Alfriend and Schaub,[3] Kang et al.,[4] among many others). The use of a group of small satellites to accomplish certain space missions will likely be less expensive than one large, complex satellite. Moreover, the satellite cluster concept minimizes risk in that the performance of the cluster may degrade gracefully in the presence of a satellite failure.

This study deals with the communication requirements necessary to enable cooperation between independent cluster members. In practice, communication between members of a satellite formation may be limited for various reasons. Various forms of interference, such as solar radiation or radio frequency interference from a satellite's thrusters, may cause errors in communication or prevent it altogether. Communication between satellites may also be delayed if channels normally used for such communication are being used for other purposes, such as exchange of command or scientific data with a ground station. Also, communication may be delayed if the data to be transmitted are temporarily unavailable. For example, if a satellite is thrusting, it may not be able to acquire reliable measurement data.

The challenge posed by controlling a satellite cluster in the presence of such communication constraints has motivated a study of decentralized control in the context of limited information exchange. The nature of this problem is characterized by the participation of multiple players, each acting on its own information set and making independent decisions, but working to fulfill a shared performance objective. The solution approach for this problem is based on the team theory concept of Radner,[5] Marshak,[6] and Marshak and Radner.[7] Specifically, Radner[5] shows that, for static team problems involving Gaussian probabilities, the unique Bayes team decision function is linear. Ho and Chu[8] have extended Radner's static team result to linear dynamic systems. Sandell and Athans[9] have combined the static team solution and a dynamic programming scheme to obtain an explicit solution for the linear-quadratic-Gaussian (LQG) stochastic control dynamic team problem with one-step-delayed information sharing pattern. This information pattern assumes that players communicate their measurements to each other with a one-step delay. Control actions are performed at every time step. Fan et al.[10] determined the counterpart solution for the linear-exponential-Gaussian dynamic team problem exhibiting the one-step-delayed information sharing pattern. The results apply for both convex and nonconvex exponential cost functions.

One contribution of this paper is to extend the dynamic team solution to the multistep delayed case. The multistep delay is made possible by defining the state of the system in the static team problem to include the random variables in all time steps involved in the delay. This redefined static team problem is then combined with a dynamic programming scheme to allow application to a dynamic team problem. This represents a modest variation of that of Ho and Chu[8] in that the state of the system is not assumed to be zero mean. It is also a modest variation of the solution of Sandell and Athans[9] in that the static team problem involves a more generalized form of the cost function.

When the approach described is used, optimal control laws are described for two communication paradigms, based on assumed linear dynamics, a quadratic performance criterion in the state and control, and additive Gaussian noise, that is, the LQG problem. The first requires sharing of control and state estimate information

Presented as Paper 2004-5023 at the AIAA Guidance, Navigation, and Control Conference, Providence, RI, 16–19 August 2004; received 3 September 2004; revision received 24 April 2005; accepted for publication 2 June 2005.

*Graduate Student, Mechanical and Aerospace Engineering Department, University of California, Los Angeles, 610 S. Main St, Suite 531, Los Angeles, CA 90014-2035. Student Member AIAA.

†Member of Technical Staff, Guidance Analysis Department, Aerospace Corporation, MS M4-971, 2350 East El Segundo Boulevard, El Segundo, CA 90245.

‡Professor, Mechanical and Aerospace Engineering Department, Box 951597, 38-137 Engineering IV. Fellow AIAA.

§Assistant Professor, Mechanical and Aerospace Engineering Department, 801 22nd Street Northwest. Senior Member AIAA.

¶Aerospace Engineer, Flight Dynamics Analysis Branch, Mission Engineering Systems Analysis Division, Code 595. Senior Member AIAA.

between players after any one of them executes a control action. The second only requires that control information be exchanged and is thought to represent the minimum information exchange necessary for an affine control solution. Both algorithms are reviewed in Sec. II following a summary of the more familiar centralized control algorithm.

The information patterns considered here are partially nested cases consistent with dynamic programming. Information patterns other than such partially nested cases lead to optimization problems that have not to this date been solved.[11]

This approach of minimizing a performance index for which an affine control solution is optimal differs from guidance rules employed in the consensus seeking literature. For example, Ren and Beard[12] construct a paradigm in which each node communicates only with its two nearest neighbors. To meet its control objectives, Ren and Beard asymptotically reduce the error in the synchronization of the coordination vectors among the nodes, along with a local tracking error based only on local information. The information exchange scheme of this approach differs from the fully connected communication topology discussed in this paper. The approach discussed in Ref. 12 and other such architectures, which reduce the interconnection between the vehicles relative to the paradigms presented in this paper, admit only adhoc decentralized controllers. Optimal control solutions such as those described in this paper can be used as a baseline for comparison of any such adhoc decentralized controllers.

A second contribution of this paper involves the application of these decentralized control algorithms to a satellite formation maintenance problem and their subsequent performance evaluation. Details regarding the application to the satellite formation control problem are addressed in Sec. III. Performance data, observations, and conclusions are contained in Secs. IV and V.

II. Review of Control Algorithms

In this section, we review the control algorithms that are the subject of this paper. First, a problem statement is given and notational conventions are introduced. This is followed by a review of the centralized control algorithm. This algorithm assumes that the controller has access to all measurement data, and will be used as a baseline for comparison of the performance of the decentralized control algorithms. Following the review of the centralized algorithm are descriptions of the decentralized algorithms and their information exchange requirements.

A. Problem Statement

Consider a dynamic, discrete-time, linear, time-varying, stochastic, l-player LQG team problem, with the following dynamics:

$$\boldsymbol{x}_{t+1} = A_t \boldsymbol{x}_t + B_t \boldsymbol{u}_t + w_t, \qquad u_t = 0 \,\forall\, t \neq \tau_i \tag{1}$$

where $t \in [0, 1, \ldots, T]$ is the time index, the state of the system at time t is represented by the n vector $\boldsymbol{x}_t$, A_t and B_t are known by all players, $w_t \sim N(0, W_t)$, and $x_0 \sim N(\bar{x}_0, M_0)$. The players are permitted to engage controls only at specified time steps, in accordance with a predetermined control schedule. Time steps in which at least one player exerts a control are designated with subscripts τ_i, where $i = 1, 2, 3 \ldots$. In general, there may be multiple time steps of inactivity between control steps at τ_i and τ_{i+1}, which will be denoted with the subscripts τ_i, $\tau_i + 1$, $\tau_i + 2, \ldots, \tau_{i+1}$. Moreover, the number of players that are permitted to control at each control step τ_i may vary and will be designated $r(\tau_i)$. Therefore, $\boldsymbol{u}_{\tau_i}$ in Eq. (1) is a vector containing all controls at a given control step,

$$\boldsymbol{u}_{\tau_i}^T = \begin{bmatrix} \boldsymbol{u}_{\tau_i}^{1^T} & \boldsymbol{u}_{\tau_i}^{2^T} & \cdots & \boldsymbol{u}_{\tau_i}^{r(\tau_i)^T} \end{bmatrix} \tag{2}$$

Each $\boldsymbol{u}_{\tau_i}^j \in \Re^{p^j}$ in Eq. (2) is the control executed by the jth player. The control coefficient matrix at τ_i in Eq. (1) is, therefore, given by

$$B_{\tau_i} = \begin{bmatrix} B_{\tau_i}^1 & B_{\tau_i}^2 & \cdots & B_{\tau_i}^{r(\tau_i)} \end{bmatrix} \tag{3}$$

At each time step, each player obtains the following measurements:

$$y_t^j = C_t^j \boldsymbol{x}_t + v_t^j, \qquad \forall j \in l \tag{4}$$

where $y_t^j \in \Re^{q^j}$ and $v_t^j \sim N(0, V_t^j)$.

The following shared performance index is to be minimized:

$$J = \sum_{t=0}^{T} \boldsymbol{x}_t^T Q_t \boldsymbol{x}_t + \sum_{i=1}^{k} \boldsymbol{u}_{\tau_i}^T R_{\tau_i} \boldsymbol{u}_{\tau_i} \tag{5}$$

where k is the number of steps at which controls are executed and $Q_t \geq 0$ and $R_{\tau_i} \geq 0$ are appropriately chosen weighting matrices.

The problem is to minimize the cost function in Eq. (5) subject to dynamics and initial conditions in Eq. (1) with local measurements in Eq. (4) taken at every time step t and controls restricted to times τ_i.

B. Centralized LQG Controller

Consider a system with linear dynamics and initial conditions identified in Eq. (1), local measurements as given in Eq. (4), and performance criterion in Eq. (5). The optimal centralized control for each player is a function of the measurement data and past controls from all players,

$$\boldsymbol{u}_{\tau_i}^j = \boldsymbol{u}_{\tau_i}^j \left(I_{\tau_i} \right) \tag{6}$$

Specifically, the optimal control is a function of current information,

$$I_{\tau_i} = \left\{ \bar{x}_0, M_0, Y_{\tau_i}, \gamma_{\tau_{i-1}} \right\} \tag{7}$$

The measurement history in Eq. (7) includes data from all players,

$$Y_{\tau_i} \equiv \bigcup_{j=1}^{l} Y_{\tau_i}^j \tag{8}$$

with $Y_{\tau_i}^j$ being the complete measurement history for the jth player, up until the current measurement,

$$Y_{\tau_i}^j \equiv \left\{ y_0^j, y_1^j, y_2^j, \ldots, y_{\tau_i}^j \right\} \tag{9}$$

The set of past controls $\gamma_{\tau_{i-1}}$ is given by

$$\gamma_{\tau_{i-1}}^T = \left[\boldsymbol{u}_{\tau_1}^T \boldsymbol{u}_{\tau_2}^T \ldots \boldsymbol{u}_{\tau_{i-1}}^T \right] \tag{10}$$

with $\boldsymbol{u}_{\tau_1}, \boldsymbol{u}_{\tau_2}, \ldots, \boldsymbol{u}_{\tau_{i-1}}$ representing all of the controls enacted at each control step up to τ_{i-1}, as defined in Eq. (2).

The general solution to this LQG problem is given in Ref. 13 as

$$\boldsymbol{u}_{\tau_i}^j = \Lambda_{\tau_i}^j \hat{\boldsymbol{x}}_{\tau_i} \tag{11}$$

where $\hat{\boldsymbol{x}}_{\tau_i}$ is the best a posteriori state estimate given all of the information up to time τ_i,

$$\hat{x}_{\tau_i} \equiv E\left[\boldsymbol{x}_{\tau_i} | I_{\tau_i} \right] \tag{12}$$

This state estimate is propagated by a discrete-time Kalman filter. The control gains are

$$\Lambda_{\tau_i}^j = -\left[R_{\tau_i}^j + B_{\tau_i}^{j^T} S_{\tau_i+1} B_{\tau_i}^j \right]^{-1} B_{\tau_i}^{j^T} S_{\tau_i+1} A_{\tau_i} \tag{13}$$

where $B_{\tau_i}^j$ is defined as in Eq. (3) and S_t is propagated backward by the Riccati equation,

$$S_t = A_t^T S_{t+1} A_t + Q_t \tag{14a}$$

for $t \neq \tau_i$, or

$$S_{\tau_i} = A_{\tau_i}^T S_{\tau_i+1} A_{\tau_i} - \sum_{j=1}^{r(\tau_i)} \Lambda_{\tau_i}^{j^T} \left(R_{\tau_i}^j + B_{\tau_i}^{j^T} S_{\tau_i+1} B_{\tau_i}^j \right) \Lambda_{\tau_i}^j + Q_{\tau_i} \tag{14b}$$

for $t = \tau_i$, with the boundary condition $S_T = Q_T$. $R_{\tau_i}^j$ in Eqs. (13) and (14b) is the weighting placed on a control executed by player j at control step τ_i in the performance criterion of Eq. (5).

C. Control and State Estimate Sharing Algorithm

Here we revisit the control and state estimate-sharing algorithm originally described by Belanger et al.[14] This paradigm requires that the individual players exchange their state estimates and control vectors after any one of them activates a control. This information must be exchanged before the next control action of any one of the players. For a thorough derivation, see Ananyev.[15]

Again, the problem is to minimize the cost function in Eq. (5) subject to dynamics and initial conditions in Eq. (1) with local measurements in Eq. (4) taken at every time step t and controls restricted to times τ_i as governed by a preset control schedule.

1. Dynamic Programming Solution

Consider the dynamic programming solution for this problem, where the optimal return function is given as

$$j^*_{\tau_{i+1}}\left(I'_{\tau_i}\right) = \min_{\gamma^{\tau_k}_{\tau_{i+1}}} E\left[J \,\middle|\, I'_{\tau_i}\right] \tag{15}$$

The expectation is conditioned on shared information up until the control step at τ_i,

$$I'_{\tau_i} = \left\{\bar{x}_0, M_0, Y_{\tau_i}, \gamma_{\tau_i}\right\} \tag{16}$$

where Y_{τ_i} is the combined measurement histories of all players up to τ_i, as defined in Eq. (8), and γ_{τ_i} are all of the past controls up to τ_i, defined as in Eq. (10). The minimization in Eq. (15) is with respect to $\gamma^{\tau_k}_{\tau_{i+1}}$, the set of all remaining controls up until the final control at step τ_k,

$$\gamma^{\tau_k}_{\tau_{i+1}} = \left\{u_{\tau_{i+1}}, u_{\tau_{i+2}}, \ldots, u_{\tau_k}\right\} \tag{17}$$

The performance index J in Eq. (15) is defined in Eq. (5).

The dynamic programming recursion rule at control step τ_i is

$$\begin{aligned} j^*_{\tau_i}\left(I'_{\tau_{i-1}}\right) = \min_{u_{\tau_i}} E\Big[\Big\{ & \boldsymbol{x}^T_{\tau_{i-1}+1} Q_{\tau_{i-1}+1} \boldsymbol{x}_{\tau_{i-1}+1} \\ & + \boldsymbol{x}^T_{\tau_{i-1}+2} Q_{\tau_{i-1}+2} \boldsymbol{x}_{\tau_{i-1}+2} + \cdots + \boldsymbol{x}^T_{\tau_i} Q_{\tau_i} \boldsymbol{x}_{\tau_i} \\ & + \boldsymbol{u}^T_{\tau_i} R_{\tau_i} \boldsymbol{u}_{\tau_i} + j^*_{\tau_{i+1}}\left(I'_{\tau_i}\right)\Big\} \Big| I'_{\tau_{i-1}}\Big] \end{aligned} \tag{18}$$

The minimization is over the control set $\boldsymbol{u}_{\tau_i}$ of all players allowed to participate at control step τ_i, as defined in Eq. (2).

2. Redefinition of the State Vector

The approach to finding the optimal control solution for Eq. (18) involves the introduction of an extended state vector, which we refer to as the state of the world. Redefinition of Eq. (18) in terms of this extended state vector will yield a static team problem similar to that addressed by Radner.[5] To this end, let us define the state of the world to be the following:

$$\boldsymbol{\eta}^T_{\tau_i|\tau_{i-1}} = \begin{bmatrix} x^T_{\tau_{i-1}+1} & w^T_{\tau_{i-1}+1} & w^T_{\tau_{i-1}+2} & \cdots & w^T_{\tau_i-1} \end{bmatrix} \tag{19}$$

where $\boldsymbol{\eta}_{\tau_i|\tau_{i-1}} \in \Re^{n(\tau_i - \tau_{i-1})}$ includes the shared state of the system just after the control action at τ_{i-1} and subsequent process noise up until just before the next control at τ_t.

The dynamics of Eq. (1) can be redefined in terms of this state of the world as follows:

$$\boldsymbol{\eta}_{\tau_{i+1}|\tau_i} = \Phi_{\tau_i|\tau_{i-1}} \boldsymbol{\eta}_{\tau_i|\tau_{i-1}} + w_{\tau_{i+1}|\tau_i} + \Gamma_{\tau_i} \boldsymbol{u}_{\tau_i} \tag{20}$$

with initial condition:

$$\boldsymbol{\eta}^T_{\tau_1|0} = \begin{bmatrix} x^T_0 & w^T_0 & \cdots & w^T_{\tau_1-1} \end{bmatrix} \tag{21}$$

where $\boldsymbol{u}_{\tau_i}$ is composed of all controls activated at time τ_i as defined in Eq. (2) and $\boldsymbol{w}_{\tau_{i+1}|\tau_i} \in \Re^{n(\tau_{i+1}-\tau_i)}$ is composed of stacked process noise vectors,

$$\boldsymbol{w}^T_{\tau_{i+1}|\tau_i} = \begin{bmatrix} \boldsymbol{w}^T_{\tau_i} & \boldsymbol{w}^T_{\tau_i+1} & \cdots & \boldsymbol{w}^T_{\tau_{i+1}-1} \end{bmatrix} \tag{22}$$

The local measurements over the interval between control actuations are governed by

$$Y^j_{\tau_i|\tau_{i-1}} = H^j_{\tau_i|\tau_{i-1}} \boldsymbol{\eta}_{\tau_i|\tau_{i-1}} + \theta^j_{\tau_i|\tau_{i-1}} \tag{23}$$

$Y^j_{\tau_i|\tau_{i-1}} \in \Re^{q^j(\tau_i - \tau_{i-1})}$ is composed of stacked local measurements going from time index $\tau_{i-1}+1$ to τ_i, as shown in Eq. (24):

$$Y^{j^T}_{\tau_i|\tau_{i-1}} = \begin{bmatrix} y^{j^T}_{\tau_{i-1}+1} & y^{j^T}_{\tau_{i-1}+2} & \cdots & y^{j^T}_{\tau_i} \end{bmatrix} \tag{24}$$

$H^j_{\tau_i|\tau_{i-1}}$ is an enlarged measurement geometry matrix of dimension $q^j(\tau_i - \tau_{i-1})$ by $n(\tau_i - \tau_{i-1})$. Here $\theta^j_{\tau_i|\tau_{i-1}}$ is composed of stacked measurement noise vectors.

The dynamic programming recursion rule in Eq. (18) can then be redefined in terms of the state of the world in Eq. (19). This yields

$$\begin{aligned} j^*_{\tau_i}(I'_{\tau_{i-1}}) = \min_{u_{\tau_i}} E\Big[\Big\{ & \eta^T_{\tau_i|\tau_{i-1}} Q_{\tau_i|\tau_{i-1}} \eta_{\tau_i|\tau_{i-1}} \\ & + u^T_{\tau_i} R_{\tau_i} u_{\tau_i} + j^*_{\tau_{i+1}}(I'_{\tau_i})\Big\} \Big| I'_{\tau_{i-1}}\Big] \end{aligned} \tag{25}$$

where $I'_{\tau_{i-1}}$ is defined as in Eq. (16) and $Q_{\tau_i|\tau_{i-1}}$ is an $n(\tau_i - \tau_{i-1})$ by $n(\tau_i - \tau_{i-1})$ matrix that contains the individual state weightings in Eq. (18).

The optimal return function $j^*_{\tau_{i+1}}(I'_{\tau_i})$ in Eq. (25) takes the form

$$\begin{aligned} j^*_{\tau_{i+1}}(I'_{\tau_i}) = & E\left[\eta^T_{\tau_{i+1}|\tau_i} L_{\tau_{i+1}} \eta_{\tau_{i+1}|\tau_i} | I'_{\tau_i}\right] \\ & + \text{control-independent terms} \end{aligned} \tag{26}$$

with $L_{\tau_{i+1}}$ determined by a backward recursion to be discussed later in this section. [See Eq. (36).]

After substituting the dynamics of Eq. (20) into Eq. (26), placing the result into Eq. (25), and doing some algebraic manipulation, one finds that the optimal cost to go at each control step τ_i takes the following form:

$$\begin{aligned} j^*_{\tau_i}(I'_{\tau_{i-1}}) = \min_{u_{\tau_i}} E\Big[\Big\{ & u^T_{\tau_i} U_{\tau_i} u_{\tau_i} + 2u^T_{\tau_i} S_{\tau_i|\tau_{i-1}} \eta_{\tau_i|\tau_{i-1}} \\ & + \text{control-independent terms}\Big\} \Big| I'_{\tau_{i-1}}\Big] \end{aligned} \tag{27}$$

Equation (27), with state of the world $\boldsymbol{\eta}$, represents a static team problem similar to that addressed by Radner.[5] The expressions for U_{τ_i} and $S_{\tau_i|\tau_{i-1}}$ are given by

$$U_{\tau_i} = R_{\tau_i} + \Gamma^T_{\tau_i} L_{\tau_{i+1}} \Gamma_{\tau_i} \tag{28}$$

$$S_{\tau_i|\tau_{i-1}} = \Gamma^T_{\tau_i} L_{\tau_{i+1}} \Phi_{\tau_i|\tau_{i-1}} \tag{29}$$

where R_{τ_i} is the weighting on the control defined in Eq. (25), $\Phi_{\tau_i|\tau_{i-1}}$ multiplies the state of the world in Eq. (20), and Γ_{τ_i} is the control coefficient matrix in Eq. (20).

3. Optimal Control Solution

Application of Radner's result yields the following optimal control law, where a total of $r(\tau_i)$ members execute controls:

$$u^{j^*}_{\tau_i} = K^j_{\tau_i} Y^j_{\tau_i|\tau_{i-1}} + G^j_{\tau_i} \bar{\eta}_{\tau_i|\tau_{i-1}} \qquad \forall j \in [1, r(\tau_i)] \tag{30}$$

where $Y^j_{\tau_i|\tau_{i-1}}$ is defined as in Eq. (24) and $\bar{\eta}_{\tau_i|\tau_{i-1}} = E[\boldsymbol{\eta}_{\tau_i|\tau_{i-1}}| I'_{\tau_{i-1}}]$. The optimal control for each member is a linear function of local measurements going back to the last control action executed by any member and the expectation of the shared state of the world defined in Eq. (19). The measurement gains $K^j_{\tau_i}$ are the unique

solutions of the following linear matrix equations:

$$U^{jj}_{\tau_i} K^j_{\tau_i} \left(H^j_{\tau_i|\tau_{i-1}} M_{\tau_i|\tau_{i-1}} H^{j^T}_{\tau_i|\tau_{i-1}} + \Theta^j_{\tau_i|\tau_{i-1}} \right) + \sum_{i \neq j,\, i=1}^{r(\tau_i)} U^{ij}_{\tau_i} K^i_{\tau_i} H^i_{\tau_i|\tau_{i-1}} M_{\tau_i|\tau_{i-1}} H^{i^T}_{\tau_i|\tau_{i-1}} = -S^j_{\tau_i|\tau_{i-1}} M_{\tau_i|\tau_{i-1}} H^{j^T}_{\tau_i|\tau_{i-1}} \qquad \forall j \in [1, r(\tau_i)] \tag{31}$$

Solutions for $K^j_{\tau_i}$ are substituted into the following equation to find the state of the world gains $G^j_{\tau_i}$:

$$\begin{bmatrix} G^1_{\tau_i} \\ G^2_{\tau_i} \\ \vdots \\ G^{r(\tau_i)}_{\tau_i} \end{bmatrix} = -U^{-1}_{\tau_i} \begin{bmatrix} \left(\sum_{j \neq 1} U^{1j}_{\tau_i} K^j_{\tau_i} H^j_{\tau_i|\tau_{i-1}} + S^1_{\tau_i|\tau_{i-1}} \right) \left[I - M_{\tau_i|\tau_{i-1}} H^{1^T}_{\tau_i|\tau_{i-1}} \left(H^1_{\tau_i|\tau_{i-1}} M_{\tau_i|\tau_{i-1}} H^{1^T}_{\tau_i|\tau_{i-1}} + \Theta^1_{\tau_i|\tau_{i-1}} \right)^{-1} H^1_{\tau_i|\tau_{i-1}} \right] \\ \left(\sum_{j \neq 2} U^{2j}_{\tau_i} K^j_{\tau_i} H^j_{\tau_i|\tau_{i-1}} + S^2_{\tau_i|\tau_{i-1}} \right) \left[I - M_{\tau_i|\tau_{i-1}} H^{2^T}_{\tau_i|\tau_{i-1}} \left(H^2_{\tau_i|\tau_{i-1}} M_{\tau_i|\tau_{i-1}} H^{2^T}_{\tau_i|\tau_{i-1}} + \Theta^2_{\tau_i|\tau_{i-1}} \right)^{-1} H^2_{\tau_i|\tau_{i-1}} \right] \\ \left(\sum_{j \neq r(\tau_i)} U^{r(\tau_i)j}_{\tau_i} K^j_{\tau_i} H^j_{\tau_i|\tau_{i-1}} + S^{r(\tau_i)}_{\tau_i|\tau_{i-1}} \right) \left[I - M_{\tau_i|\tau_{i-1}} H^{r(\tau_i)^T}_{\tau_i|\tau_{i-1}} \left(H^{r(\tau_i)}_{\tau_i|\tau_{i-1}} M_{\tau_i|\tau_{i-1}} H^{r(\tau_i)^T}_{\tau_i|\tau_{i-1}} + \Theta^{r(\tau_i)}_{\tau_i|\tau_{i-1}} \right)^{-1} H^{r(\tau_i)}_{\tau_i|\tau_{i-1}} \right] \end{bmatrix} \tag{32}$$

Equations (31) and (32) are derived from the results of Radner,[5] Ho and Chu,[8] and Sandell and Athans[9] as adapted to the multistep delayed case. The a priori variances $M_{\tau_i|\tau_{i-1}}$ in Eqs. (31) and (32), are defined by

$$M_{\tau_i|\tau_{i-1}} = E\left[\{\eta_{\tau_i|\tau_{i-1}} - \bar{\eta}_{\tau_i|\tau_{i-1}}\} \{\eta_{\tau_i|\tau_{i-1}} - \bar{\eta}_{\tau_i|\tau_{i-1}}\}^T \,\middle|\, I_{\tau_{i-1}} \right] \tag{33}$$

$\Theta^j_{\tau_i|\tau_{i-1}}$ in Eqs. (31) and (32) is a $q^j\,(\tau_i - \tau_{i-1})$ by $q^j\,(\tau_i - \tau_{i-1})$ matrix with $\Theta^j_{\tau_i|\tau_{i-1}} = E[\theta^j_{\tau_i|\tau_{i-1}} \theta^{j^T}_{\tau_i|\tau_{i-1}}]$. Finally, U_{τ_i} and $S_{\tau_i|\tau_{i-1}}$ are expanded as

$$U_{\tau_i} = \begin{bmatrix} U^{11}_{\tau_i} & U^{12}_{\tau_i} & \cdots & U^{1r(\tau_i)}_{\tau_i} \\ U^{21}_{\tau_i} & U^{22}_{\tau_i} & \cdots & U^{2r(\tau_i)}_{\tau_i} \\ \vdots & \vdots & \ddots & \vdots \\ U^{r(\tau_i)1}_{\tau_i} & U^{r(\tau_i)2}_{\tau_i} & \cdots & U^{r(\tau_i)r(\tau_i)}_{\tau_i} \end{bmatrix} \tag{34}$$

$$S^T_{\tau_i|\tau_{i-1}} = \begin{bmatrix} S^{1^T}_{\tau_i|\tau_{i-1}} & S^{2^T}_{\tau_i|\tau_{i-1}} & \cdots & S^{r(\tau_i)^T}_{\tau_i|\tau_{i-1}} \end{bmatrix} \tag{35}$$

Note that $\bar{\eta}_{\tau_i|\tau_{i-1}}$ in Eq. (30) is constructed using locally maintained state estimates that would have been exchanged since the last control step at time τ_{i-1}. A low-power scheme for propagation and exchange of local state estimates, such as that described by Wolfe and Speyer,[16] may be used for this purpose.

The matrix L in Eqs. (26), (28), and (29) is propagated backward as follows:

$$L_{\tau_i} = 2\left[G^T_{\tau_i} \left(U_{\tau_i} K_{\tau_i} H_{\tau_i|\tau_{i-1}} + S_{\tau_i|\tau_{i-1}} + \tfrac{1}{2} U_{\tau_i} G_{\tau_i} \right) + \tfrac{1}{2} H^T_{\tau_i|\tau_{i-1}} K^T_{\tau_i} U_{\tau_i} K_{\tau_i} H_{\tau_i|\tau_{i-1}} + H^T_{\tau_i|\tau_{i-1}} K_{\tau_i} S_{\tau_i|\tau_{i-1}} \right] + \Phi^T_{\tau_i|\tau_{i-1}} L_{\tau_{i+1}} \Phi_{\tau_i|\tau_{i-1}} + Q_{\tau_i|\tau_{i-1}} \tag{36}$$

where $Q_{\tau_i|\tau_{i-1}}$ is the state of the world weighting referenced in Eq. (25) and

$$K_{\tau_i} = \begin{bmatrix} K^1_{\tau_i} & 0 & \cdots & 0 \\ 0 & K^2_{\tau_i} & \cdots & 0 \\ \vdots & \vdots & \ddots & \vdots \\ 0 & 0 & \cdots & K^{r(\tau_i)}_{\tau_i} \end{bmatrix}, \qquad H_{\tau_i|\tau_{i-1}} = \begin{bmatrix} H^1_{\tau_i|\tau_{i-1}} \\ H^2_{\tau_i|\tau_{i-1}} \\ \vdots \\ H^{r(\tau_i)}_{\tau_i|\tau_{i-1}} \end{bmatrix} \tag{37}$$

Equation (36) has the terminal condition $L_T = Q_{T|\tau_k}$, where τ_k is the last control step before the terminal time T.

In summary, the optimal control law is found by solving a static team problem that occurs at each control step τ_i of the dynamic programming process. The static team problem is defined in terms of the state of the world shown in Eq. (19). The form of the optimal control shown in Eq. (30) is linear in the local measurements taken since the last information exchange and the last shared state estimate. This, of course, requires that the players remember all measurement information that has been collected since the last communication.

The control schedule for this dynamic team problem is allowed to be most irregular: Any individual player may execute a control action at any time step, or be passive for as long as it has to. However, the dynamic programming solution process requires that the control schedule be known in advance by all players for the duration of their cooperation.

D. Control (only)-Sharing Algorithm

We now examine a decentralized control algorithm that assumes only control information is shared between players. This paradigm requires that an individual player broadcast its control vector when it activates that control. This transmission must occur before the next control action of any one of the players. The result is reduced information exchange but a higher expected cost when compared to the control and state estimate-sharing algorithm earlier. Note that the control-sharing paradigm represents what is thought to be the minimum information exchange necessary for an affine control law. For a thorough derivation of this algorithm, see Ananyev.[15]

Again, the problem is to minimize the cost function in Eq. (5) subject to dynamics and initial conditions in Eq. (1) with local measurements in Eq. (4) taken at every time step t and controls restricted to times τ_i as governed by a preset control schedule.

1. *Dynamic Programming Solution*

Consider the dynamic programming solution for this problem, where the optimal return function is given as

$$j^*_{\tau_{i+1}}(I''_{\tau_i}) = \min_{\gamma^{\tau_k}_{\tau_i+1}} E\left[J \,|\, I''_{\tau_i} \right] \tag{38}$$

The expectation is conditioned on the shared information

$$I''_{\tau_i} = \left\{ \bar{x}_0, M_0, \gamma_{\tau_i} \right\} \tag{39}$$

Because only controls are shared in this algorithm, the shared information in Eq. (39) differs from its counterpart in Eq. (16). In Eq. (39) γ_{τ_i} are all of the past controls, defined as in Eq. (10). The minimization in Eq. (38) is with respect to $\gamma^{\tau_k}_{\tau_{i+1}}$, which are all of the remaining controls up until the final control step τ_k as given in Eq. (17). The performance index J in Eq. (38) is defined in Eq. (5).

The dynamic programming recursion rule at control step τ_i is

$$j^*_{\tau_i}(I''_{\tau_{i-1}}) = \min_{u_{\tau_i}} E\left[\left\{ \sum_{t=\tau_{i-1}+1}^{\tau_i} x^T_t Q_t x_t + u^T_{\tau_i} R_{\tau_i} u_{\tau_i} + j^*_{\tau_{i+1}}(I''_{\tau_i}) \right\} | I''_{\tau_{i-1}} \right] \tag{40}$$

2. Redefinition of the State Vector

Once again, finding the optimal control solution for Eq. (40) involves the introduction of an extended state vector. Redefinition of Eq. (40) in terms of this revised state of the world yields a static team problem similar to that addressed by Radner.[5] Suppose the state of the world of Eq. (19) is modified to include terms going back to the initial time, as follows:

$$\boldsymbol{\eta}_{\tau_i}^T = \lfloor x_0^T \quad w_0^T \quad w_1^T \quad \cdots \quad w_{\tau_i-1}^T \rfloor \tag{41}$$

As defined in Eq. (41), $\boldsymbol{\eta}_{\tau_i} \in \Re^{n(\tau_i+1)}$ includes the shared initial condition and subsequent process noise up until just before the control at τ_i. Note that, if defined this way, the size of the state of the world increases as one progresses forward in time. The dynamic programming recursion rule of Eq. (40) can be rewritten in terms of the state of the world as follows:

$$\begin{aligned} j_{\tau_i}^*(I''_{\tau_i-1}) &= \min_{u_{\tau_i}} E\Big[\Big\{\eta_{\tau_i}^T Q_{\tau_i}\eta_{\tau_i} + u_{\tau_i}^T R_{\tau_i} u_{\tau_i} + 2\gamma_{\tau_i-1}^T \tilde{S}_{\tau_i}\eta_{\tau_i} \\ &\quad + \gamma_{\tau_i-1}^T \tilde{R}_{\tau_i}\gamma_{\tau_i-1} + j_{\tau_i+1}^*(I''_{\tau_i})\Big\}\Big| I''_{\tau_i-1}\Big] \\ &= \min_{u_{\tau_i}} E\Big[\Big\{\eta_{\tau_i}^T L_{\tau_i}\eta_{\tau_i} + 2u_{\tau_i}^T S'_{\tau_i}\eta_{\tau_i} + u_{\tau_i}^T U_{\tau_i} u_{\tau_i} \\ &\quad + 2u_{\tau_i}^T U'_{\tau_i}\gamma_{\tau_i-1} + 2\gamma_{\tau_i-1}^T S''_{\tau_i}\eta_{\tau_i} + \gamma_{\tau_i-1}^T \tilde{U}_{\tau_i}\gamma_{\tau_i-1}\Big\}| I''_{\tau_i-1}\Big] \end{aligned} \tag{42}$$

The minimization is over the control set $\boldsymbol{u}_{\tau_i}$ of all players allowed to participate at control step τ_i, as defined in Eq. (2). The weightings in Eq. (42) are given by

$$\begin{aligned} L_{\tau_i} &= Q_{\tau_i} + \bar{L}_{\tau_i+1}[1 : n\cdot(\tau_i+1), 1 : n\cdot(\tau_i+1)] \\ S''_{\tau_i} &= \bar{S}_{\tau_i} + \bar{S}_{\tau_i+1}\big[1 : \text{size}\big(\gamma_{\tau_i-1}\big), 1 : n\cdot(\tau_i+1)\big] \\ \tilde{U}_{\tau_i} &= \tilde{R}_{\tau_i} + \bar{U}_{\tau_i+1}\big[1 : \text{size}\big(\gamma_{\tau_i-1}\big), 1 : \text{size}\big(\gamma_{\tau_i-1}\big)\big] \\ U_{\tau_i} &= R_{\tau_i} + \bar{U}_{\tau_i+1}\big[\text{size}\big(u_{\tau_i}\big), \text{size}\big(u_{\tau_i}\big)\big] \\ S'_{\tau_i} &= \bar{S}_{\tau_i+1}\big[\text{size}\big(u_{\tau_i}\big), 1 : n\cdot(\tau_i+1)\big] \\ U'_{\tau_i} &= \tfrac{1}{2}\big[\bar{U}_{\tau_i+1}\big[\text{size}\big(u_{\tau_i}\big), 1 : \text{size}\big(\gamma_{\tau_i-1}\big)\big] \\ &\quad + \bar{U}_{\tau_i+1}^T\big[1 : \text{size}\big(\gamma_{\tau_i-1}\big), \text{size}\big(u_{\tau_i}\big)\big]\big] \end{aligned} \tag{43}$$

The parenthetical expressions in Eqs. (43) represent the partitions of the corresponding matrices to be used in the calculation. For example, in the construction of L_{τ_i}, the elements in $\bar{L}_{\tau_i+1}$ containing information corresponding to the first τ_i time steps are used. This is a square matrix with $n(\tau_i+1)$ elements on a side, n being the dimension of the state vector in Eq. (1). In other cases, matrix partitions containing information corresponding to all of the past controls up to control step τ_{i-1} are used; yet others use information corresponding only to the current control at step τ_i. Thus, the quantities in Eqs. (43) shrink in size as one propagates backward to reflect the shrinking state of the world as defined in Eq. (41) and decreasing number of past controls as defined in Eq. (10).

The optimal return function, $j_{\tau_i+1}^*(I''_{\tau_i})$ in Eq. (42) can be expressed in the form

$$\begin{aligned} j_{\tau_i+1}^*(I''_{\tau_i}) = \min_{u_{\tau_i+1}} E\Big[\Big\{&\eta_{\tau_i+1}^T \bar{L}_{\tau_i+1}\eta_{\tau_i+1} \\ &+ \gamma_{\tau_i}^T \bar{U}_{\tau_i+1}\gamma_{\tau_i} + 2\gamma_{\tau_i}^T \bar{S}_{\tau_i+1}\eta_{\tau_i+1}\Big\}| I''_{\tau_i}\Big] \end{aligned} \tag{44}$$

where $\bar{L}_{\tau_i+1}$, $\bar{U}_{\tau_i+1}$, and $\bar{S}_{\tau_i+1}$ are governed by backward propagations to be specified later in this section [Eqs. (55–57)].

Because the past controls are assumed to be transmitted noiselessly and are, therefore, perfectly known, they can be treated as constants. The information structure for each player can then be expressed as follows:

$$Y_{\tau_i}^j = H_{\tau_i}^j \boldsymbol{\eta}_{\tau_i} + \theta_{\tau_i}^j + \bar{R}_{\tau_i}^j \gamma_{\tau_i-1} \tag{45}$$

$Y_{\tau_i}^j \in \Re^{q^j(\tau_i+1)}$ in Eq. (45) is composed of stacked local measurements going from the initial time forward to time τ_i, as follows:

$$Y_{\tau_i}^{j^T} = \lfloor y_0^{j^T} \quad y_1^{j^T} \quad \cdots \quad y_{\tau_i}^{j^T} \rfloor \tag{46}$$

$H_{\tau_i}^j$ is an enlarged measurement geometry matrix having $q^j(\tau_i+1)$ rows and $n(\tau_i+1)$ columns. In Eq. (45), $\theta_{\tau_i}^j$ is composed of stacked measurement noise vectors. Finally, $\bar{R}_{\tau_i}^j$ defines the impact of the past control set γ_{τ_i-1} [Eq. (10)] on $Y_{\tau_i}^j$.

3. Optimal Control Solution

Application of Radner's result[5] to the static team problem defined by Eq. (42) yields an optimal control of the form

$$\boldsymbol{u}_{\tau_i}^{j^*} = K_{\tau_i}^j Y_{\tau_i}^j + G_{\tau_i}^j \bar{\boldsymbol{\eta}}_{\tau_i} + b_{\tau_i}^j \gamma_{\tau_i-1} \qquad \forall j \in [1, r(\tau_i)] \tag{47}$$

with $Y_{\tau_i}^j$ and γ_{τ_i-1} defined in Eqs. (46) and (10), respectively, and $\bar{\boldsymbol{\eta}}_{\tau_i} = E[\eta_{\tau_i}|\bar{x}_0, M_0]$. The optimal control in the control (only) sharing algorithm is a linear function of local measurements going back to the initial time, the expectation of the shared state of the world defined in Eq. (41), and all of the earlier controls. The measurement gains $K_{\tau_i}^j$ are the unique solutions of the following linear matrix equations:

$$\begin{aligned} &U_{\tau_i}^{jj} K_{\tau_i}^j \Big(H_{\tau_i}^j M_{\tau_i} H_{\tau_i}^{j^T} + \Theta_{\tau_i}^j\Big) + \sum_{i\neq j, i=1}^{r(\tau_i)} U_{\tau_i}^{ij} K_{\tau_i}^i H_{\tau_i}^i M_{\tau_i} H_{\tau_i}^{i^T} \\ &\quad = -S'^j_{\tau_i} M_{\tau_i} H_{\tau_i}^{j^T} \forall j \in [1, r(\tau_i)] \end{aligned} \tag{48}$$

Solutions for $K_{\tau_i}^j$ are substituted to find the state of the world gains $G_{\tau_i}^j$,

$$G_{\tau_i} = \begin{bmatrix} G_{\tau_i}^1 \\ G_{\tau_i}^2 \\ \vdots \\ G_{\tau_i}^{r(\tau_i)} \end{bmatrix} = -U_{\tau_i}^{-1} \begin{bmatrix} \Big(\sum_{j\neq 1} U_{\tau_i}^{1j} K_{\tau_i}^j H_{\tau_i}^j + S'^1_{\tau_i}\Big)\Big[I - M_{\tau_i} H_{\tau_i}^{1^T}\Big(H_{\tau_i}^1 M_{\tau_i} H_{\tau_i}^{1^T} + \Theta_{\tau_i}^1\Big)^{-1} H_{\tau_i}^1\Big] \\ \Big(\sum_{j\neq 2} U_{\tau_i}^{2j} K_{\tau_i}^j H_{\tau_i}^j + S'^2_{\tau_i}\Big)\Big[I - M_{\tau_i} H_{\tau_i}^{2^T}\Big(H_{\tau_i}^2 M_{\tau_i} H_{\tau_i}^{2^T} + \Theta_{\tau_i}^2\Big)^{-1} H_{\tau_i}^2\Big] \\ \vdots \\ \Big(\sum_{j\neq r(\tau_i)} U_{\tau_i}^{r(\tau_i)j} K_{\tau_i}^j H_{\tau_i}^j + S'^{r(\tau_i)}_{\tau_i}\Big)\Big[I - M_{\tau_i} H_{\tau_i}^{r(\tau_i)^T}\Big(H_{\tau_i}^{r(\tau_i)} M_{\tau_i} H_{\tau_i}^{r(\tau_i)^T} + \Theta_{\tau_i}^{r(\tau_i)}\Big)^{-1} H_{\tau_i}^{r(\tau_i)}\Big] \end{bmatrix} \tag{49}$$

Note that Eqs. (48) and (49) have exactly the same form as their counterparts in Eqs. (31) and (32); the change in time indices reflects the redefinition of the state of the world $\boldsymbol{\eta}$ to include elements going

back to the initial time. Finally, the gain on the past controls, $b^j_{\tau_i}$, can be found from

$$\begin{bmatrix} b^1_{\tau_i} \\ b^1_{\tau_i} \\ \vdots \\ b^{r(\tau_i)}_{\tau_i} \end{bmatrix} = -U^{-1}_{\tau_i}\left(U'_{\tau_i} - D_{\tau_i}\bar{R}_{\tau_i}\right) \tag{50}$$

where

$$D_{\tau_i} = \begin{bmatrix} \left(\sum_{j\neq 1} U^{1j}_{\tau_i} K^j_{\tau_i} H^j_{\tau_i} + S'^1_{\tau_i}\right) M_{\tau_i} H^{1^T}_{\tau_i} \left(H^1_{\tau_i} M_{\tau_i} H^{1^T}_{\tau_i} + \Theta^1_{\tau_i}\right)^{-1} - U^{12}_{\tau_i} K^2_{\tau_i} \cdots - U^{1r(\tau_i)}_{\tau_i} K^{r(\tau_i)}_{\tau_i} \\ -U^{21}_{\tau_i} K^1_{\tau_i} \left(\sum_{j\neq 2} U^{2j}_{\tau_i} K^j_{\tau_i} H^j_{\tau_i} + S'^2_{\tau_i}\right) M_{\tau_i} H^{2^T}_{\tau_i} \left(H^2_{\tau_i} M_{\tau_i} H^{2^T}_{\tau_i} + \Theta^2_{\tau_i}\right)^{-1} \cdots - U^{2r(\tau_i)}_{\tau_i} K^{r(\tau_i)}_{\tau_i} \\ \vdots \qquad\qquad \vdots \qquad\qquad \ddots \qquad\qquad \vdots \\ -U^{r(\tau_i)1}_{\tau_i} K^1_{\tau_i} \qquad -U^{r(\tau_i)2}_{\tau_i} K^2_{\tau_i} \cdots \left(\sum_{j\neq r(\tau_i)} U^{r(\tau_i)j}_{\tau_i} K^j_{\tau_i} H^j_{\tau_i} + S'^{r(\tau_i)}_{\tau_i}\right) M_{\tau_i} H^{r(\tau_i)^T}_{\tau_i} \left(H^{r(\tau_i)}_{\tau_i} M_{\tau_i} H^{r(\tau_i)^T}_{\tau_i} + \Theta^{r(\tau_i)}_{\tau_i}\right)^{-1} \end{bmatrix} \tag{51}$$

Equations. (48–51) are derived from the results of Radner,[5] Ho and Chu,[8] and Sandell and Athans[9] as adapted to the multistep delayed case. U_{τ_i}, U'_{τ_i}, and S'_{τ_i} in Eqs. (48–51) are defined in Eqs. (43). Partitions of U_{τ_i}, S'_{τ_i}, and $\bar{R}_{\tau_i}$ are referenced according to the following scheme:

$$U_{\tau_i} = \begin{bmatrix} U^{11}_{\tau_i} & U^{12}_{\tau_i} & \cdots & U^{1r(\tau_i)}_{\tau_i} \\ U^{21}_{\tau_i} & U^{22}_{\tau_i} & \cdots & U^{2r(\tau_i)}_{\tau_i} \\ \vdots & \vdots & \ddots & \vdots \\ U^{r(\tau_i)1}_{\tau_i} & U^{r(\tau_i)2}_{\tau_i} & \cdots & U^{r(\tau_i)r(\tau_i)}_{\tau_i} \end{bmatrix} \tag{52}$$

$$S'_{\tau_i} = \begin{bmatrix} S'^1_{\tau_i} \\ S'^2_{\tau_i} \\ \vdots \\ S'^{r(\tau_i)}_{\tau_i} \end{bmatrix}, \qquad \bar{R}_{\tau_i} = \begin{bmatrix} \bar{R}^1_{\tau_i} \\ \bar{R}^2_{\tau_i} \\ \vdots \\ \bar{R}^{r(\tau_i)}_{\tau_i} \end{bmatrix} \tag{53}$$

with $\bar{R}^j_{\tau_i}$ defined in Eq. (45). $H^j_{\tau_i}$ in Eqs. (48–51) is defined as in Eq. (45). $\Theta^j_{\tau_i} = E[\theta^j_{\tau_i}\theta^{j^T}_{\tau_i}]$ with $\theta^j_{\tau_i}$ also defined as in Eq. (45). M_{τ_i} is given by

$$M_{\tau_i} = E\left[\{\eta_{\tau_i} - \bar{\eta}_{\tau_i}\}\{\eta_{\tau_i} - \bar{\eta}_{\tau_i}\}^T | M_0\right] \tag{54}$$

As mentioned earlier, the matrices $\bar{L}, \bar{U}$, and $\bar{S}$ in the optimal return function [Eq. (44)] are governed by backward propagations. These propagations are defined as follows:

$$\bar{L}_{\tau_i} = 2G^T_{\tau_i}\left(U_{\tau_i} K_{\tau_i} H_{\tau_i} + S'_{\tau_i} + \tfrac{1}{2} U_{\tau_i} G_{\tau_i}\right) + L_{\tau_i} + 2H^T_{\tau_i} K^T_{\tau_i} S'_{\tau_i} + H^T_{\tau_i} K^T_{\tau_i} U_{\tau_i} K_{\tau_i} H_{\tau_i} \tag{55}$$

$$\bar{U}_{\tau_i} = 2\bar{R}^T_{\tau_i}\left(\tfrac{1}{2} D^T_{\tau_i} U^{-1}_{\tau_i} D_{\tau_i} + K^T_{\tau_i} D_{\tau_i} + \tfrac{1}{2} K^T_{\tau_i} U_{\tau_i} K_{\tau_i}\right)\bar{R}_{\tau_i} - U'^T_{\tau_i} U^{-1}_{\tau_i} U'_{\tau_i} + \tilde{U}_{\tau_i} \tag{56}$$

$$\bar{S}_{\tau_i} = \bar{R}^T_{\tau_i}\left(K^T_{\tau_i} + D^T_{\tau_i} U^{-1}_{\tau_i}\right)\left(U_{\tau_i} K_{\tau_i} H_{\tau_i} + S'_{\tau_i} + U_{\tau_i} G_{\tau_i}\right) - U'^T_{\tau_i} U^{-1}_{\tau_i} S'_{\tau_i} + S''_{\tau_i} \tag{57}$$

with

$$K_{\tau_i} = \begin{bmatrix} K^1_{\tau_i} & 0 & \cdots & 0 \\ 0 & K^2_{\tau_i} & \cdots & 0 \\ \vdots & \vdots & \ddots & \vdots \\ 0 & 0 & \cdots & K^{r(\tau_i)}_{\tau_i} \end{bmatrix} \tag{58}$$

$$H^T_{\tau_i} = \begin{bmatrix} H^{1^T}_{\tau_i} & H^{2^T}_{\tau_i} & \cdots & H^{r(\tau_i)^T}_{\tau_i} \end{bmatrix} \tag{59}$$

$\bar{R}_{\tau_i}$, D_{τ_i}, and G_{τ_i} in Eqs. (55–57) are defined in Eqs. (53), (51), and (49), respectively. All other quantities are defined in Eqs. (43). The initial conditions for these backward propagations are derived from the expression

$$j^*_T(I''_{\tau_k}) = E\left[\sum_{\tau_k+1}^{T} \boldsymbol{x}^T_t Q_t \boldsymbol{x}_t \,\middle|\, I''_{\tau_k}\right] = E\left[\left\{\eta^T_T \bar{L}_T \eta_T + \gamma^T_{\tau_k} \bar{U}_T \gamma_{\tau_k} + 2\gamma^T_{\tau_k} \bar{S}_T \eta_T\right\} \middle| I''_{\tau_k}\right] \tag{60}$$

where T is the final time, τ_k is the last control step, and γ_{τ_k} is the set of all controls from initial to final time, defined as in Eq. (10). $\bar{L}, \bar{U}$, and $\bar{S}$ shrink as they are propagated backward to accommodate the shrinking size of the state of the world $\boldsymbol{\eta}_{\tau_i}$ and shrinking number of past controls, $\gamma_{\tau_{i-1}}$.

4. *Augmented Control-Sharing Algorithm*

Because the control (only) sharing algorithm severely limits coordination between cluster members, its application to the satellite formation control problem was considered to be impractical. Because state estimates are not exchanged between cluster members, each member must use shared control values to extrapolate the position of the other members using linear dynamic models. Application of such an algorithm in a nonlinear environment would leads to degraded performance. Moreover, this algorithm poses a large computational and storage burden because the number of calculations involved is a function of the size of the state of the world.

For the purposes of the performance testing described in Sec. IV, a modified version of the control-sharing algorithm is employed, where state estimates are exchanged in between control-sharing sessions. Information exchange is still less than the control and state estimate-sharing algorithm, and the size of the control-sharing sessions can be set as required by the satellite cluster mission. A distributed linear estimator, such as that described by Wolfe and Speyer,[16] can be used to generate the shared global state estimates that are used to form the initial conditions for each control-sharing session.

III. Application to Satellite Cluster Problem

We discuss the application of the preceding control algorithms to a satellite cluster problem. Whereas the control algorithms described in the preceding section can be applied to any number of cooperating satellites, a scenario involving the control of a cluster of three satellites moving around an elliptic reference orbit was chosen

as a representative satellite cluster problem. The following section details the setup of the problem.

A. Frenet Frame State Transition Matrix

For reasons that will become evident, it is desirable to have satellite dynamics expressed in terms of coordinate axes that are tangential and perpendicular to the reference orbital path. We refer to this as the Frenet frame because the axes correspond to the Frenet coordinate system (see Ref. 17). The origin of the Frenet frame is a point on the reference orbital path (hereafter called the reference point) that moves as if it were a satellite. The y axis of the Frenet frame is aligned with the velocity vector of the reference point. The x axis is normal to the reference orbit at the reference point. The z axis is out of plane.

Carter[18] gives a state transition matrix for relative motion linearized about an elliptic orbit. His result is given in terms of true anomaly ν and assumes a different coordinate frame. Moreover, his dynamics are scaled by $\sqrt{\omega}$, where $\omega = \mathrm{d}\nu/\mathrm{d}t$. Because unscaled time-based Frenet frame dynamics are desired, a similarity transform of the following form is necessary:

$$\bar{T}(\nu_{t+1}, \nu_t) = P(\nu_{t+1}) T(\nu_{t+1}, \nu_t) P^{-1}(\nu_t) \tag{61}$$

$T(\nu_{t+1}, \nu_t)$ in Eq. (61) represents Carter's transition matrix of relative motion linearized about an elliptic orbit, defined based on true anomalies at time t and $t+1$. $P(\nu_{t+1})$ and $P^{-1}(\nu_t)$ contain transformations given by Carter to perform the $1/\sqrt{\omega}$ scaling and adjust to time-based dynamics. They also contain rotations to the desired Frenet frame. $\bar{T}(\nu_{t+1}, \nu_t)$ is the resultant Frenet frame transition matrix.

B. State-Space Model of the Satellite Cluster

The discrete-time state vector for the cluster combines the Frenet frame state vectors for the cluster members.

$$\boldsymbol{x}_t^T = \begin{bmatrix} \boldsymbol{x}_t^{1^T} & \boldsymbol{x}_t^{2^T} & \boldsymbol{x}_t^{3^T} \end{bmatrix} \tag{62}$$

The superscripts 1, 2, and 3 refer to the cluster member satellites. The Frenet frame state vector for each satellite is

$$\boldsymbol{x}_t^{j^T} = \begin{bmatrix} x_t^j & \dot{x}_t^j & y_t^j & \dot{y}_t^j & z_t^j & \dot{z}_t^j \end{bmatrix} \tag{63}$$

The superscript j refers to the satellite number in the cluster and t refers to the time index. Thus, the state vector for the cluster is composed of the Frenet frame positions and velocities of each of the cluster members.

The full control vector consists of the control vectors for the three satellites.

$$\boldsymbol{u}_t^T = \begin{bmatrix} \boldsymbol{u}_t^{1^T} & \boldsymbol{u}_t^{2^T} & \boldsymbol{u}_t^{3^T} \end{bmatrix} \tag{64}$$

where

$$\boldsymbol{u}_t^{j^T} = \begin{bmatrix} u_{xt}^j & u_{yt}^j & u_{zt}^j \end{bmatrix} \tag{65}$$

If the control thrusts are modeled as instantaneous changes in velocity, the control coefficient matrix simply consists of the velocity columns of the state transition matrix.

The cluster dynamic equation is then

$$\begin{aligned} \boldsymbol{x}_{t+1} &= \begin{bmatrix} \bar{T}^1(\nu_{t+1}, \nu_t) & 0 & 0 \\ 0 & \bar{T}^2(\nu_{t+1}, \nu_t) & 0 \\ 0 & 0 & \bar{T}^3(\nu_{t+1}, \nu_t) \end{bmatrix} \boldsymbol{x}_t \\ &\quad + \begin{bmatrix} \bar{B}^1(\nu_{t+1}, \nu_t) & 0 & 0 \\ 0 & \bar{B}^2(\nu_{t+1}, \nu_t) & 0 \\ 0 & 0 & \bar{B}^3(\nu_{t+1}, \nu_t) \end{bmatrix} \boldsymbol{u}_t \\ &= \bar{A}_t \boldsymbol{x}_t + \bar{B}_t \boldsymbol{u}_t \end{aligned} \tag{66}$$

where

$$\bar{T}^1(\nu_{t+1}, \nu_t) = \bar{T}^2(\nu_{t+1}, \nu_t) = \bar{T}^3(\nu_{t+1}, \nu_t) \tag{67}$$

$$\bar{B}^1(\nu_{t+1}, \nu_t) = \bar{B}^2(\nu_{t+1}, \nu_t) = \bar{B}^3(\nu_{t+1}, \nu_t) \tag{68}$$

C. Model for Local Measurements

It is assumed that each satellite in the formation is able to measure directly its own Frenet frame state. Therefore, the measurement model for each satellite consists of its local state vector plus additive Gaussian noise,

$$\boldsymbol{y}_t^j = I_6 \boldsymbol{x}_t^j + \boldsymbol{v}_t^j \tag{69}$$

where $\boldsymbol{v}_i^j$ is a random vector with statistics $\boldsymbol{v}_t^j \sim N\left(0, V_t^j\right)$. This measurement model does not allow a satellite to obtain measurements about another satellite's state. However, the satellite cluster simulation has been implemented assuming that shared relative measurements are available to all satellites at predetermined times. Details of this implementation are discussed in Sec. IV.

D. Cost Function

There are three simultaneous considerations that govern the control laws:

1) The cluster members should be in a specified relative geometry when the reference point reaches a certain value of true anomaly, ν_f. This requirement is inspired by the performance of many current Earth science missions, in which much of the science is done on only a small portion of the orbit.

2) When the reference point is at ν_f, the cluster members should be positioned such that their centroid lies on the reference orbit (but is not necessarily constrained to be at the reference point). This means that the Frenet x and z components of the centroid location should be minimized, but y will be free.

3) Weight the control effort over the entire mission.

Based on the preceding criteria, the specific cost function to be used in the satellite cluster problem is expressed in terms of the perturbations of the Frenet frame state from preset nominal trajectories at ν_f, $\Delta\bar{x}(\nu_f)$, as well as control effort at times τ_i, u_{τ_i},

$$\begin{aligned} J &= \Delta\bar{x}^T(\nu_f)[Q_{xc}(\nu_f) + Q_{zc}(\nu_f) + Q_d(\nu_f) \\ &\quad + I\varepsilon]\Delta\bar{x}(\nu_f) + \sum_{i=1}^{k} u_{\tau_i}^T R_{\tau_i} u_{\tau_i} \end{aligned} \tag{70}$$

The nominal trajectory for each satellite is an unpowered Keplerian trajectory that would ideally satisfy the performance criteria. Q_{xc} and Q_{zc} in Eq. (70) are the weightings on perturbations of the x and z components of the cluster centroid from their nominal locations at ν_f. The weighting on relative distances between cluster members, Q_d, consists of the following components:

$$Q_d = \Psi^T q_d \Psi \tag{71}$$

where Ψ is the Jacobian resulting from the linearization of the expressions for relative distance between each of the cluster members about the nominal trajectory at ν_f. In Eq. (71), q_d contains weightings for each of the relative distance components. Note that the weightings on the centroid and relative distance criteria are only enforced at ν_f.

The final term in Eq. (70) is a weighting on aggregate control effort throughout the simulation, with u_{τ_i} representing all controls activated at control step τ_i as defined in Eq. (2) and k being the total number of control steps.

Note that the $I\varepsilon$ term is the identity matrix multiplied by a small positive number and is added to preserve the positive definiteness properties of the control Riccati matrices defined in Eqs. (14), (36), and (55–57). Without this weighting, such positive definiteness properties may be affected by numerical instabilities in the backward propagations; a small value of $\varepsilon = 10^{-6}$ as used for the simulations discussed in this paper. Note that an ε a couple orders of magnitude smaller was found to result in drastically degraded

performance, whereas larger ε were found to lead to only slightly improved performance.

IV. Simulation Setup and Results

In this section, the control algorithms presented in Sec. II are performance tested in a nonlinear motion simulation of a cluster of three satellites. Performance of the decentralized algorithms is compared to that of the centralized LQG controller having access to the current measurements of all satellites. The controllers to be examined are based on the linear dynamics described in Sec. III and treat unmodeled dynamics as zero mean Gaussian random disturbances. However, the satellite cluster simulation provides a nonlinear dynamic environment including disturbing J_2 effects.

A. Performance Criteria

In the simulations to be discussed, the satellite cluster is propagated around one full orbit, starting at perigee. It is desired that the cluster be in a predetermined formation on return to perigee. This formation requirement is balanced against a simultaneous weighting on control effort.

The predetermined formation is based on centroid and relative distance criteria as discussed in the preceding section. Specifically, in the desired formation, the satellites are to be in a straight line, with the outer satellites each being 141.421 m from the middle satellite.

Table 1 shows the relative weightings used in penalizing the components of the cost function in Eq. (70). Fuel usage is weighted heavily due to the premium placed on fuel in space missions. The other weightings were found to yield good performance through some trial and error. A relatively small centroid weighting was sufficient because the centroid position is just a linear combination of the positions of the cluster members. As such, it is relatively easy for the controller to position the cluster centroid appropriately. However, because relative distances are linearized in the cost function, it is necessary to weight them heavily to avoid invalidating that linearization.

Finally, note that velocities are not considered in the evaluation of cluster performance.

B. Control Schedule

All three control algorithms to be considered, the control and state estimate-sharing algorithm, the control-only-sharing algorithm, and the centralized algorithm, will adhere to the same control schedule in these simulations. This control schedule calls for the reference orbit to be split into 40 steps of equal true anomaly. Measurements will be taken at each of these steps. Controls will be activated by all cluster members simultaneously at every other step. This allows for 41 measurements (including the measurements at the initial time) and 20 control steps over the course of the orbit. As was mentioned earlier, only one orbit will be simulated for the purposes of this performance evaluation.

C. Initial State Uncertainty

When the simulation starts at perigee, the initial Frenet frame state of the cluster is set by adding position and velocity perturbations to what would be the ideal satellite positions. These initial perturbations are modeled as Gaussian random vectors. The standard deviations of the perturbations are 50 m for Frenet frame positions and 1 mm/s for velocities.

D. Measurement Uncertainty

The satellite cluster simulation is implemented using local absolute Frenet frame measurements as well as shared relative position measurements. Models used for local absolute measurements taken at every true anomaly step are of the linear form shown in Eq. (69), where the uncertainties are Gaussian random vectors. Absolute measurement uncertainties are zero mean with standard deviations of 1 m for position measurements and 4 cm/s for velocity measurements. In addition to exchanging local absolute state estimate information, the cluster satellites exchange relative position measurements. These relative measurements are assumed to be read as vector quantities defined in terms of the Frenet coordinate system. They are indexed at the same time as the exchanged local absolute state estimates and are used to enhance the global state estimate derived from blending the exchanged state estimates together. These relative position measurements are modeled with an additive Gaussian uncertainty that is zero mean with standard deviation of 2 cm. The uncertainties used here for both absolute and relative measurements are based on uncertainties associated with code and carrier-phase global positioning system (GPS) measurements as determined from past experimental results.[19,20] The experiments described in Refs. 19 and 20 were conducted using a GPS simulator and a car test. Carrier-phase and code measurements were double differenced. Double differencing was used to eliminate biases and clock differences, whereas single differencing eliminates common errors such as ephemeris errors. These experiments used an Ashtech Z12 two-channel receiver, where the integers were resolved using widelane techniques. After resolving the integers, a least-squares routine was applied to the carrier-phase measurements to produce the relative position estimates. These position estimates and the associated error variances are used in a loosely coupled manner as the noisy relative GPS position measurements for our controller. When the geometry of the orbits involved is considered modeling these uncertainties as being the same for all cluster members and constant throughout the orbit can be regarded as a decent first-order approximation for the purposes of the satellite cluster simulations.

Table 1 Cost function weightings

Cost criteria	Weighting
Centroid position	0.1
Relative distances	1
Fuel usage	1

The shared relative position measurements are used to update a shared global state estimate that is formed as a result of the exchange of absolute Frenet frame state estimates between cluster members. A distributed linear estimator, such as that described by Wolfe and Speyer,[16] can be used to combine local compressed data vectors that are shared at desired times. As a result of this combination, each cluster member has the same global state estimate. The timing of the exchange of absolute and relative Frenet frame information occurs at times specified by the decentralized control algorithms, as described in Sec. II. The error covariances associated with both absolute and relative measurements are assumed to be known by all cluster members and are factored into the propagation of local conditional mean estimates.

It has been shown that the use of GPS measurements does not always provide for accurate estimation of the orbit semimajor axis or orbital energy.[21,22] In Refs. 23 and 24 it is shown, that the Kalman filter using a loosely coupled GPS estimator does not have a strong negative correlation between position and velocity errors. It is anticipated that the filters employed in this demonstration of these decentralized control algorithms will suffer as well, which can impact performance. However, the fact that the controller for each cluster member incorporates a local measurement sequence in a batched form may alleviate this difficulty.

The remainder of this section involves comparison of the control algorithms by running simulations over three different reference orbits. Note that the reference orbits include J_2. This was done so that the controllers do not have to fight bulk J_2 disturbances to meet the formation centroid criteria at the end of the orbit. Description of the first reference orbit follows.

E. First Reference Orbit

The first simulation is for a roughly equatorial (inclination $\sim$1 deg) reference orbit with low eccentricity ($e \sim 0.1$). The characteristics of this reference orbit are shown in Table 2.

Table 3 shows errors in meeting objectives for performance criteria of interest, averaged over 1000 Monte Carlo runs. Included are average errors in the centroid and relative distance criteria that were discussed earlier in this section. The average cost is a calculation based on Eq. (70) with the weightings as given in Table 1. Average

Table 2 First reference orbit characteristics

Parameter	Value
Eccentricity	∼0.1
Radius at perigee	6800 km
Radius at apogee	8400 km
Inclination	1 deg
Right ascension of the ascending node	270 deg
Argument of perigee	90 deg
Period	∼6594 s

Table 3 Errors in meeting performance criteria, first reference orbit

Cost parameter	Centralized	Control and state estimate sharing	Augmented control sharing
Frenet x centroid error, m	0.348	0.368	0.500
Frenet z centroid error, m	0.290	0.308	0.386
Relative distance error, satellites 1 and 2, m	0.083	0.281	1.625
Relative distance error, satellites 1 and 3, m	0.132	0.306	1.967
Relative distance error, satellites 2 and 3, m	0.130	0.303	1.286
Fuel usage satellite 1, m/s	0.207	0.216	0.222
Fuel usage satellite 2, m/s	0.206	0.214	0.209
Fuel usage satellite 3, m/s	0.206	0.215	0.211
Average cost	0.137	0.475	13.019

total fuel usage per satellite for the duration of the simulation is also given.

F. Second Reference Orbit

The second reference orbit simulated has greater eccentricity than the first ($e \sim 0.32$). The characteristics of the second reference orbit are shown in Table 4. Sets of results, averaged over 1000 Monte Carlo runs, are shown in Tables 5 and 6 for two different inclinations: Table 5 for a roughly equatorial orbit (inclination ∼0.1 deg) and Table 6 for an inclination of 30 deg.

G. Observations

The relative performance of the control algorithms as shown in Tables 3, 5, and 6 generally support our expectations. The centralized algorithm tends to exhibit the best performance because it assumes full access to all satellites' absolute and relative measurements

Table 4 Second reference orbit characteristics

Parameter	Value
Eccentricity	∼0.32
Radius at perigee	6900 km
Radius at apogee	13400 km
Right ascension of the ascending node	270 deg
Argument of perigee	90 deg
Period	∼10177 s

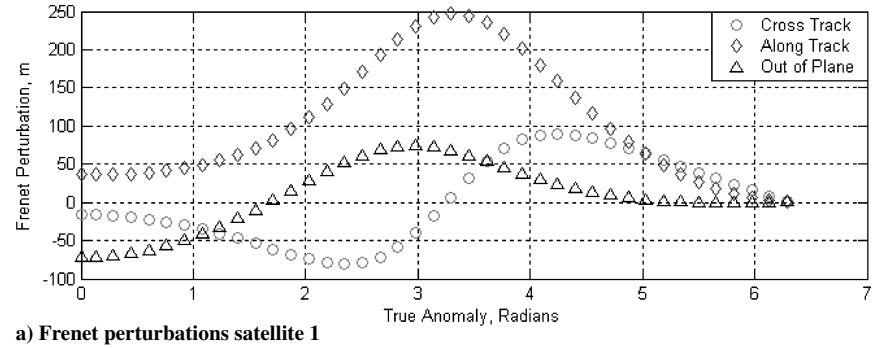

a) Frenet perturbations satellite 1

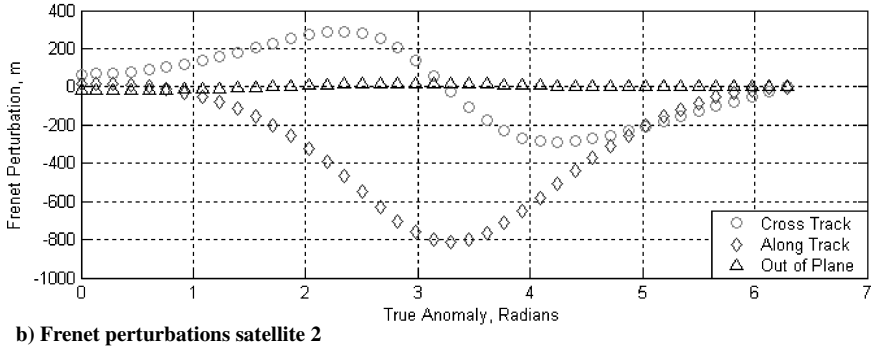

b) Frenet perturbations satellite 2

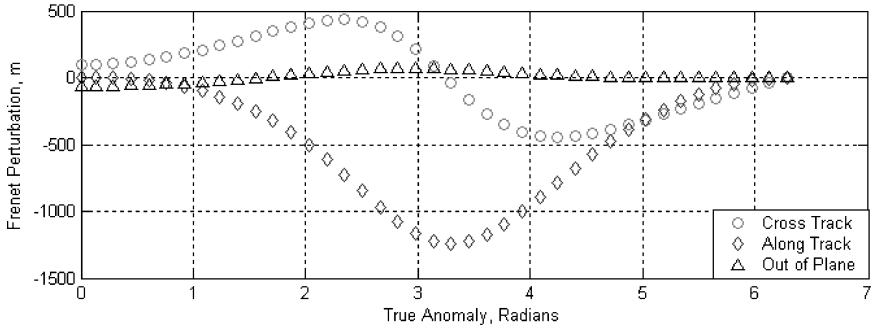

c) Frenet perturbations satellite 3

Fig. 1 Frenet position errors.

at every true anomaly step. The control and state estimate-sharing algorithm provides intermediate performance due to the exchange of controls, state estimates, and relative measurements with every control step. In the augmented control-sharing algorithm used in these simulations, controls are always exchanged but absolute state estimates and relative position measurements are only exchanged after every second control. Because this algorithm employs the least information exchange, it is no surprise that it exhibits the worst performance. As a matter of fact, considering the degraded performance of the augmented control-sharing algorithm, one may conclude that the slightly reduced information exchange may not be enough justification for its use in this particular application. Access to current shared information is important in determining the crucial final control action. In the centralized algorithm, this final control is a function of current shared information. Thus, the controller can make a good decision about how to position the satellites in the desired formation at the end of the orbit. However, in the control and state estimate-sharing algorithm, the final control decisions are made based on shared data that is a couple of true anomaly steps old. Because of this, nonlinear dynamics and J_2

Table 5 Errors in meeting performance criteria, second reference orbit, inclination 0.1 deg

Cost parameter	Centralized	Control and state estimate sharing	Augmented control sharing
Frenet x centroid error, m	0.334	0.348	0.448
Frenet z centroid error, m	0.284	0.295	0.372
Relative distance error, satellites 1 and 2, m	0.039	0.224	1.482
Relative distance error, satellites 1 and 3, m	0.072	0.242	1.793
Relative distance error, satellites, 2 and 3, m	0.070	0.235	1.168
Fuel usage satellite 1, m/s	0.178	0.191	0.189
Fuel usage satellite 2, m/s	0.177	0.189	0.178
Fuel usage satellite 3, m/s	0.179	0.191	0.181
Average cost	0.065	0.301	10.866

Table 6 Errors in meeting performance criteria, second reference orbit, inclination 30 deg

Cost parameter	Centralized	Control and state estimate sharing	Augmented control sharing
Frenet x centroid error, m	0.334	0.346	0.457
Frenet z centroid error, m	0.284	0.294	0.371
Relative distance error, satellites 1 and 2, m	0.060	0.249	1.484
Relative distance error, satellites 1 and 3, m	0.085	0.256	1.798
Relative distance error, satellites 2 and 3, m	0.082	0.254	1.174
Fuel usage satellite 1, m/s	0.178	0.190	0.190
Fuel usage satellite 2, m/s	0.177	0.189	0.179
Fuel usage satellite 3, m/s	0.179	0.191	0.181
Average cost	0.073	0.347	10.933

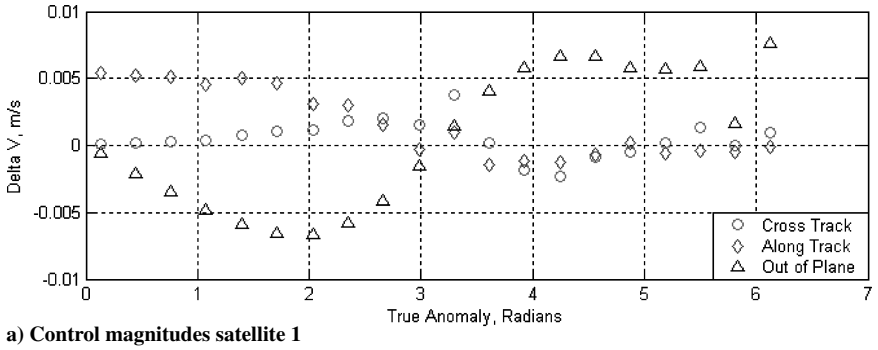

a) Control magnitudes satellite 1

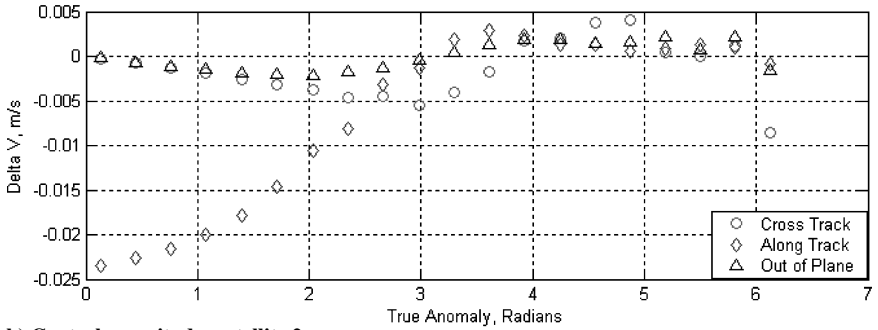

b) Control magnitudes satellite 2

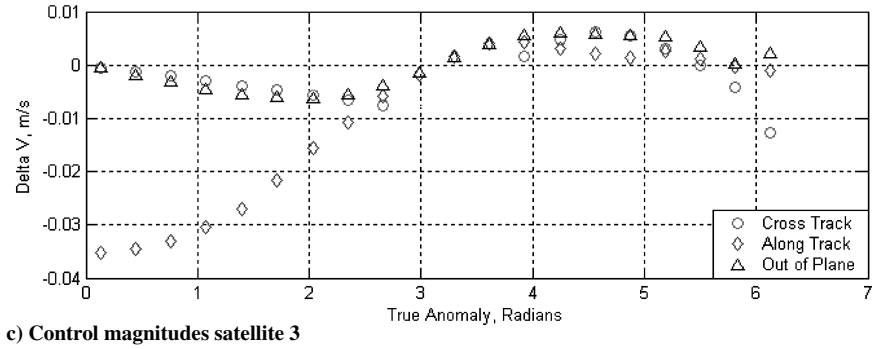

c) Control magnitudes satellite 3

Fig. 2 Control impulses.

effects that are not anticipated by the controller will have a greater effect on the position of the formation at the end of the orbit. In the augmented control-sharing case, the situation is even worse because the final control decision is based on shared information that is four true anomaly steps out of date. Thus, the relevance of shared information has an undeniable effect on the suitability of the final control commands in assembling the formation and, therefore, the overall performance of the control algorithm.

When the preceding observations are considered, it should be noted that the results are expected to be highly dependent on the control schedule used. In particular, it is expected that the difference between the algorithms' performance would be minimized by placing more control actions closer to the end of the orbit. If the augmented control-sharing algorithm was modified to allow more frequent information exchanges and control actuations toward the end of the orbit, it is expected that its performance would be much improved.

In all cases, cluster satellites come within a couple meters of desired formation targets. However, performance generally seems to be degraded when J_2 forces become more of a factor. This is evidenced by comparison of the performance data in Table 3 to those shown in Tables 5 and 6. Note the worse overall performance shown in Table 3. The fact that the reference orbit corresponding to Table 3 has lower altitude results in increased J_2 forces, which explains this observation.

Fuel usage between control algorithms appears to be roughly equal in every test case, with the centralized case exhibiting the least fuel usage by a small margin.

Figure 1 shows the deviation of each satellite from its preestablished nominal trajectory over the course of the simulation. The perturbations appear to be periodic, indicating that they are the result of J_2 forces and other unmodeled dynamics.

Figure 2 shows a pattern of control actuation that is representative of the behavior of the control algorithms studied. Again, note that the pattern of control actuation appears to be largely periodic, with large initial thrusts to counteract initial position offsets and spikes at the final control step to place the cluster satellites in the desired positions. As Chichka et al.[25] note, unmodeled dynamics are assumed in the controller design to be zero mean Gaussian process noise. However, in the satellite cluster motion simulation, dynamics not accounted for in the controller derivation include J_2 and other unmodeled higher-order effects. These effects tend to be cyclic rather than random. This attempt to model periodic dynamics with a random disturbance would explain the periodic behavior seen in the perturbations and control actuations.

Note that the preceding simulations do not incorporate the occurrence of a communications fault in the process of information sharing. In the event of such a fault, it is conceivable that a contingency plan could be followed where each satellite's control action would be a function of the best data that it has available at the time. It is expected that such an algorithm would provide degraded performance relative to the no-fault case.

Because the decentralized guidance laws allow cluster members to operate autonomously over significant intervals on the orbit, fault detection algorithms can be independently employed by each satellite. Although the formulation presented here does not include a large set of satellite sensors and actuators, the results by Chen et al.[26] show that a fault can be detected and identified in at most a few seconds. If such a fault detection scheme were to be implemented in the context of the decentralized guidance laws discussed in this paper, there would be time to identify and compensate for a faulty sensor before a control action is required.

V. Summary

The satellite cluster concept is receiving increased attention, due to its applicability in space missions involving interferometric observation and possible cost savings vs the use of one large and complex satellite. This paper reviews two separate decentralized control algorithms with an emphasis on minimizing information exchange between cluster members. Both control algorithms involve the solution of a static team problem at each backward propagation of a dynamic programming scheme. The static team solutions enable a multistep delay between collection of local sensor data and exchange of these data with other cluster members, a capability achieved through redefinition of the state vector in the static team problem. The first algorithm requires the exchange of control and state estimate information between members whenever one or more of them executes a control actuation. The second algorithm requires only that cluster members broadcast their control values on execution of a control action. This second algorithm is believed to represent the minimum information exchange that will support an affine control law.

The control and state estimate-sharing algorithm, and an augmented version of the control- (only-) sharing algorithm, where periods of control only sharing are nested between state estimate exchanges, were each evaluated in a satellite cluster simulation that employs nonlinear dynamics and J_2 perturbations. Performance objectives required that the cluster assume a given formation after one full orbit; a penalty function with simultaneous weightings referenced to formation-keeping ability and control effort was used to quantify performance. Generally speaking, the more information exchange, the better the performance. The relevance of shared information appears to become an important factor near the end of the orbit, where the cluster members attempt to assume the required formation. Because performance is affected by J_2 and other unmodeled dynamics, the robustness of the algorithms becomes increasingly tested as simulations are run-over orbits with greater J_2 effects. As is noted by Chichka et al.,[25] the effects of these unmodeled dynamics may be reduced by the introduction of a rejection filter into the control algorithms.

Acknowledgments

This work was funded under Cooperative Agreement NCC5-726 through the NASA Goddard Space Flight Center Formation Flying NASA Research Announcement. G. M. Belanger has conducted this study under the NASA Graduate Student Researchers Program.

References

[1]Chichka, D. F., "Satellite Clusters with Constant Apparent Distribution," *Journal of Guidance, Control, and Dynamics*, Vol. 24, No. 1, 2001, pp. 117–122.

[2]Hughes, S., and Hall, C., "Optimal Configurations for Rotating Spacecraft Formations," *Journal of the Astronautical Sciences*, Vol. 48, No. 2–3, 2000, pp. 225–247.

[3]Alfriend, K. T., and Schaub, H., "Dynamics and Control of Spacecraft Formations: Challenges and Some Solutions," *Journal of the Astronautical Sciences*, Vol. 48, No. 2–3, 2000, pp. 249–267.

[4]Kang, W., Sparks, A., and Banda, S., "Coordinated Control of Multisatellite Systems," *Journal of Guidance, Control, and Dynamics*, Vol. 24, No. 2, 2001, pp. 360–368.

[5]Radner, R., "Team Decision Problems," *Annals of Mathematical Statistics*, Vol. 33, Sept. 1962, pp. 857–881.

[6]Marshak, J., "Elements for a Theory of Teams," *Management Science*, Vol. 1, No. 2, 1955, pp. 127–137.

[7]Marshak, J., and Radner, R., *The Economic Theory of Teams*, Yale Univ. Press, New Haven, CT, 1972.

[8]Ho, Y. -C., and Chu, K.-G., "Team Decision Theory and Information Structures in Optimal Control Problems-Part I," *IEEE Transactions on Automatic Control*, Vol. AC-17, Feb. 1972, pp. 15–22.

[9]Sandell, N., and Athans, M., "Solution of Some Nonclassical LQG Stochastic Decision Problems," *IEEE Transactions on Automatic Control*, Vol. AC-19, No. 2, and 1974, pp. 108–116.

[10]Fan, C. -H., Speyer, J. L., and Jaensch, C. R., "Centralized and Decentralized Solutions of the Linear-Exponential-Gaussian Problem," *IEEE Transactions on Automatic Control*, Vol. 39, No. 10, 1994, pp. 1986–2003.

[11]Witsenhausen, H. S., "A Counterexample in Stochastic Optimum Control," *SIAM Journal on Control*, Vol. 6, No. 1, 1968, pp. 131–147.

[12]Ren, W., and Beard, R., "Decentralized Scheme for Spacecraft Formation Flying via the Virtual Structure Approach," *Journal of Guidance, Control, and Dynamics*, Vol. 27, No. 1, 2004, pp. 73–82.

[13]Bryson, A. E., and Ho, Y.-C., *Applied Optimal Control*, Hemisphere, Washington DC, 1975, Chap. 14.

[14]Belanger, G., Ananyev, S., Chichka, D. F., and Speyer, J. L., "Decentralized Control of Satellite Clusters Under Limited Communication," AIAA Paper 2003-5443, Aug. 2002.

[15]Ananyev, S., "Decentralized Control of Distributed Systems with Relaxed Communication," M.S. Thesis, Dept. of Mechanical and Aerospace Engineering, Univ. of California, Los Angeles, CA, Oct. 2001.

[16]Wolfe, J. D., and Speyer, J. L., "A Low-Power Filtering Scheme for Distributed Sensor Networks," *Proceedings of the 42nd IEEE Conference on Decision and Control*, Vol. 6, IEEE, Piscataway, NJ, 2003, pp. 6325, 6326.

[17]O'Neill, B., *Elementary Differential Geometry*, 2nd ed., Academic Press, London, 1997, p. 57.

[18]Carter, T. E., "State Transition Matrices for Terminal Rendezvous Studies: Brief Survey and New Example," *Journal of Guidance, Control, and Dynamics*, Vol. 21, No. 1, 1998, pp. 148–155.

[19]Abdel-Hafez, M. F., Lee, Y. J., Williamson, W. R., Wolfe, J. D., and Speyer, J. L., "A High-Integrity and Efficient GPS Integer Ambiguity Resolution Method," *Journal of the Institute of Navigation*, Vol. 50, No. 4, 2003–2004, pp. 295–310.

[20]Wolfe, J. D., Williamson, W. R., and Speyer, J. L., "Hypothesis Testing for Resolving Integer Ambiguity in GPS," *Journal of the Institute of Navigation*, Vol. 50, No. 1, 2003, pp. 45–56.

[21]Carpenter, J. R., and Schiesser, E. R., "Semimajor Axis Knowledge and GPS Orbit Determination," *Journal of the Institute of Navigation*, Vol. 48, No. 1, 2001, pp. 57–68.

[22]Carpenter, J. R., and Alfriend, K. T., "Navigation Accuracy Guidelines for Orbital Formation Flying," AIAA Paper 2003-5443, 2003.

[23]How, J. P., Alfriend, K. T., Breger, L., and Mitchell, M., "Semimajor Axis Estimation Strategies," *2nd International Symposium on Formation Flying Missions and Technologies*, Sept. 2004.

[24]Mitchell, M., Breger, L., How, J. P., and Alfriend, K. T., "Effects of Navigation Filter Properties on Formation Flying Control," AIAA Paper 2004-5024, 2004.

[25]Chichka, D. F., Belanger, G., and Speyer, J. L., "Control of Satellite Clusters in Elliptic Orbit with Limited Communication," *Annals of the New York Academy of Sciences*, edited by E. Belbruno, D. Folta, and P. Gurfil, Vol. 1017, New York Academy of Sciences, New York, 2004, pp. 177–189.

[26]Chen, R. H., Ng, H. K., Speyer, J. L., Guntur, L. S., and Carpenter, J. R., "Health Monitoring of a Satellite System," AIAA Paper 2004-5121, 2004.